AERO2000 – First Int. Conf. of the Iranian Aerospace Society, Sharif Univ. of Tech., Dec 30, 00 - Jan 1, 01.

Dynamic Crack Propagation Analysis Using A Contact Based Discontinuum Approach

S. Mohammadi*

Department of Civil Engineering, University of Tehran
Tel: +98-21-611 2273, Email: smoham@shafagh.ut.ac.ir

Abstract.

A novel approach, based on the discontinuum concepts of the Discrete Element Method, is presented for dynamic crack propagation analysis. The method is capable of analysing progressive fracturing and fragmentation behaviour as well as potential post cracking interactions caused by the newly created crack sides and segments. The method is applicable for meshed polygon systems in which each individual face may be considered as a potential contactor in the contact detection procedure. The imminence of a material crack is monitored by an anisotropic Hoffman model. To avoid the mesh dependency of the results, a bilinear local softening model is also adopted in this study to account for release of energy and redistribution of forces which caused the formation of a crack. A special remeshing method has been developed to geometrically model an individual crack by splitting the element, separating the failed node, creating new nodes and dividing the neighbouring elements to preserve the compatibility conditions. It also plays an important role in avoiding excess distortions of the finite elements in the vicinity of cracks. Several numerical simulations have been performed to assess the performance of the proposed algorithm which covers a variety of benchmark finite element tests, standard experimental data and practical applications.

Keywords: Crack Propagation, Contact Mechanics, Discontinuity, Discrete Element Method.

1 Introduction

The phenomenon of failure by catastrophic crack propagation poses problems in all applications, particularly in the aerospace industry in which safety is of paramount importance, but where over-design carries heavy penalties in terms of excess weight. Therefore, the development of reliable models for determining the failure behaviour of growing advanced materials are vitally important.

Numerical simulation of arbitrary shaped components is traditionally performed by the finite element techniques, which is rooted in the concepts of continuum mechanics and is not suited to general fracture propagation and fragmentation problems. In contrast,

*Assistant Professor

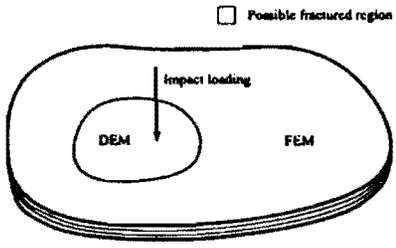

Figure 1: A Combined FE/DE model

the discrete element method (DEM) is specifically designed to solve problems that exhibit strong discontinuities in material and geometric behaviour [1]. The *discrete element method* idealizes the whole medium into an assemblage of individual bodies, which in addition to their own deformable response, interact with each other (through a contact type interaction) to capture the characteristics of the discontinuum and to perform the same response as the medium itself.

In this paper, some of the main aspects of crack initiation/propagation procedures by DEM are discussed. Testing some of the benchmark and practical problems will help in verifying the performance of the proposed algorithm

2 Discontinuum Modelling

Figure 1 shows a typical combined FE/DE model for a plate subjected to an impact loading. In a combined FE/DE method, the (predicted) fractured region is modelled using a discrete element mesh and the remainder of the specimen is modelled by a standard finite element mesh. A combined mesh enables us to prevent unnecessary contact detection and interaction calculations which comprise a major part of the analysis time [2].

Material fracture may result in the creation of new discrete bodies which are in contact and friction interaction with neighbouring bodies. A special remeshing algorithm is adopted to maintain compatibility conditions in newly fractured regions.

From the computational point of view, the discrete element procedure comprises three steps: object representation, contact detection, and contact interaction. The first two steps are closely associated to each other and are usually discussed within the framework of the contact detection algorithms. In this papaer, however, we are only concerned with the third step; contact interaction.

2.1 Contact Interaction

Once the possibility of contact between discrete bodies is detected, another method has to be used to satisfy the impenetrability condition of the bodies. The penalty method is probably the most appropriate scheme for adopting into an explicit contact analysis. In this method, penetration of the contactor object is used to establish the contact forces between contacting objects at any given time (See Figure 3).

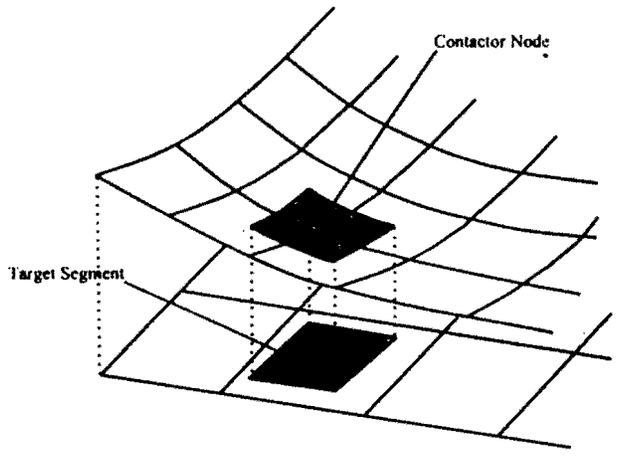

Figure 2: A general node to face contact algorithm.

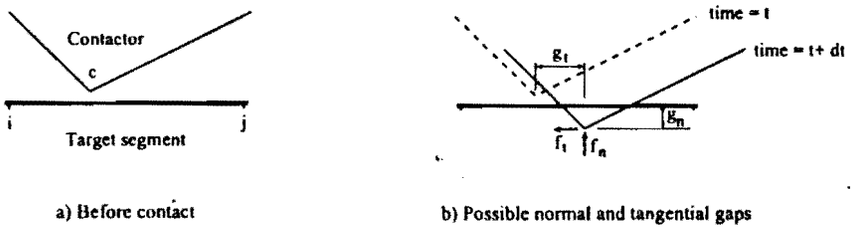

Figure 3: Contact force based on impenetrability.

The spatial version of the weak form of the dynamic boundary value problem for any admissible displacement variation $\delta \mathbf{u}$ may be defined as

$$\int_\Omega \delta\epsilon(\boldsymbol{u}) : \boldsymbol{\sigma}(\boldsymbol{u}) dv + \int_\Omega \delta\boldsymbol{u} \cdot \rho\ddot{\boldsymbol{u}} dv = \int_\Omega \delta\boldsymbol{u} \cdot \boldsymbol{f}^{\text{body}} dv + \int_{\Gamma_\sigma} \delta\boldsymbol{u} \cdot \boldsymbol{f}^{\text{surf}} da + \int_{\Gamma_c} \delta\mathbf{g}(\boldsymbol{u}) \cdot \boldsymbol{f}^{\text{con}} da \tag{1}$$

where $\boldsymbol{\sigma}$ is the Cauchy stress tensor, ϵ is the strain tensor, $\boldsymbol{u}$ is the displacement vector, while $\mathbf{g}$ represents the contact gap vector corresponding to a penalty formulation of contact interaction. Standard finite element discretisation of the variational form (2) results in the discrete set of algebraic time dependent equations which may be expressed in component form as [3, 4]:

$$\delta W^c = f_k^c \, \delta g_k = f_k^c \frac{\partial g_k}{\partial u_i^s} \delta u_i^s \tag{2}$$

where $k = n, t$ and $i = x, y$, and u_i^s is the i-component of the displacement vector at node s, $\mathbf{g} = (g_n, g_t)$ is the relative motion (gap) vector, and $\boldsymbol{f}^c$ is the contact force vector over the contact area A^c,

$$\boldsymbol{f}^c = A^c \, \boldsymbol{\sigma}^c \tag{3}$$

$$\sigma^c = \alpha\, g = \begin{bmatrix} \alpha_n & 0 \\ 0 & \alpha_t \end{bmatrix} \begin{bmatrix} g_n \\ g_t \end{bmatrix} \tag{4}$$

where α is the penalty term matrix. The contact force has to be distributed to the target and the contactor nodes.

3 Material Model

The imminence of material failure is monitored by the orthotropic Hoffman criterion, where a geometric yield surface is constructed from three tensile strengths σ_T, three compressive strengths σ_C, and three shear strengths σ_S. It may be defined as:

$$\Phi = \frac{1}{2}\boldsymbol{\sigma}^T \boldsymbol{P}\boldsymbol{\sigma} + \boldsymbol{\sigma}^T \boldsymbol{p} - \bar{\sigma}^2(\kappa) \tag{5}$$

where the projection matrix $\boldsymbol{P}$, and the projection vector $\boldsymbol{p}$ are defined based on the nine material yield strengths and a normalised yield strength $\bar{\sigma}$ (see Schellekens *et al.* [5]), and κ is a softening/hardening parameter.

4 Crack Propagation

Forming a crack is followed by releasing energy and redistributing the forces which caused the initiation of the crack. If this procedure happens immediately after occurrence of a crack, it will lead to inaccurate solutions, and more importantly, to results that strongly depend on the size of the finite elements used in the analysis.

Having recognised the serious limitation of stress-based softening failure criteria, we could move to methods directly involving fracture mechanics. An alternative procedure, pioneered by Hilleborg *et al.*, is to introduce a softening stress-strain relationship which is related to the fracture energy. In this way, fracture mechanics is indirectly introduced [6]. In the following, both methods for considering the load transfer in cracked regions will be examined

4.1 Fracture Mechanics

In this method, a complex mixed mode fracture, including modes *I*, *II*, and even *III* may be simultaneously activated. A simple criterion that governs crack growth could be presented by a linear interpolation of the energy release rates of all three modes [7].

However, since this method requires a re-analysis of the whole model in each step, it is not suitable for an explicit dynamic analysis of multiple crack problems adopted in this study. It is certainly not applicable in highly progressive fracturing and fragmentation processes [8].

4.2 Strain Softening Model

The main concept is the assumption that the fracture energy release G_f, is a material property (fracture toughness) rather than a local stress-strain curve. The implementation of the $G_f = Const.$ concept, leads to the important conclusion that the local strain-softening law depends on a fracturing zone with characterization length, l_c, depending on the finite element mesh.

One model that provides a simple approach to localization zone simulation is the bilinear Rankine softening plasticity model [1] (See Figure 4).

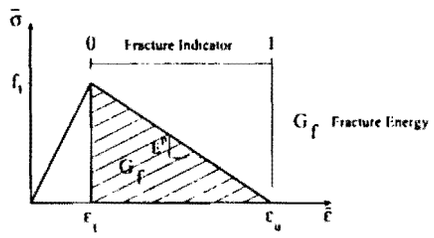

Figure 4: Fracture energy softening model.

The fracture energy release is defined as the integral of the area under the softening branch of the stress-strain curve

$$G_f = \left[\frac{1}{2} f_t (\epsilon_u - \epsilon_t)\right] l_c \tag{6}$$

where f_t is the tensile strength and ϵ_u and ϵ_t are the tensile fracture and ultimate strains respectively, and l_c is the characteristic length. The introduction of the characteristic length, l_c, is a result of expressing the fracture energy of a smeared crack model by a discrete crack model (Figure 5). The fracture energy G_f for a discrete crack of width w can be expressed as

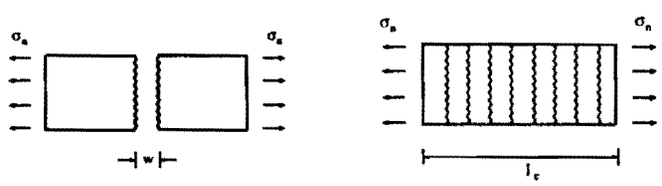

Figure 5: Discrete and smeared crack models.

$$G_f = \int \sigma_n dw \tag{7}$$

while for a smeared crack model, w is smeared across the width l_c

$$g_f = \int \sigma_n d\epsilon^{cr} \tag{8}$$

where ϵ^{cr} is the equivalent crack strain smeared over l_c

$$\epsilon^{cr} = \frac{w}{l_c} \tag{9}$$

Therefore, (8), (7) with the help of (9) gives,

$$G_f = l_c \cdot g_f \tag{10}$$

which is equivalent to (6) for the adopted strain softening model. n general, l_c is contained within one element, however the stress state that causes the crack in the discrete crack model is inclined to the local axis of the finite element, and therefore, the characteristic length will not be the finite element width. Hence, as a close approximation, it may be defined based on the area A, or the volume of the fractured element, V, [9]

$$\begin{aligned} l_c &= A^{\frac{1}{2}} \qquad for\ 2D \\ l_c &= V^{\frac{1}{3}} \qquad for\ 3D \end{aligned} \tag{11}$$

The softening modulus is then defined as

$$E^p = \frac{f_t^2\, l_c}{2G_f} \tag{12}$$

The position of the stress point on the softening branch, or the value of the fracture indicator (Figure 4), could be used as a measure, being compared to a predefined maximum value, to quantify the level of material damage for different regions.

4.2.1 Higher Modes of Fracture

There have been enormous contribution to the literature reporting on the effects of different fracture modes on the crack growth due to various loading conditions [10, 11].

The simplest mixed mode of fracture is a linear combination of the separate modes,

$$\left(\frac{G_I}{G_{cI}}\right) + \left(\frac{G_{II}}{G_{cII}}\right) = 1 \tag{13}$$

where G is the energy release rate, and G_c is the fracture toughness of the material. The general form of the mixed model, may then be expressed as

$$\left(\frac{G_I}{G_{cI}}\right)^{\frac{\alpha}{2}} + \left(\frac{G_{II}}{G_{cII}}\right)^{\frac{\alpha}{2}} = 1 \tag{14}$$

The linear model is achieved by $\alpha = 2$, and $\alpha = 4$ leads to the quadratic mixed model.

A damage mechanics model [6] is required to establish the evolution of the stress strain relationship. For the purpose of implementation in a finite element code, a damage model proposed by Mi *et al.* [12] is adopted, which can be written as

$$\bar{\boldsymbol{\sigma}} = [\boldsymbol{I} - \boldsymbol{D}]\,\boldsymbol{E}_0\bar{\boldsymbol{\epsilon}} = \left[\boldsymbol{I} - \frac{\kappa}{1+\kappa}\boldsymbol{F}\right]\boldsymbol{E}_0\bar{\boldsymbol{\epsilon}} \tag{15}$$

where $\bar{\sigma}$ and $\bar{\epsilon}$ denote stress and strain (or traction and relative displacement) along the interface with opening mode I and shearing mode II, respectively,

$$\bar{\boldsymbol{\sigma}} = \left\{ \begin{array}{c} \bar{\sigma}_I \\ \bar{\sigma}_{II} \end{array} \right\} \tag{16}$$

$$\bar{\boldsymbol{\epsilon}} = \left\{ \begin{array}{c} \bar{\epsilon}_I \\ \bar{\epsilon}_{II} \end{array} \right\} \tag{17}$$

and $\boldsymbol{E}_0$ is a diagonal stiffness matrix of the interface layer

$$\boldsymbol{E}_0 = Diag\left[\frac{f_t}{\epsilon_t}\right] \tag{18}$$

and the matrix $\boldsymbol{F}$ takes the form of

$$\boldsymbol{F} = Diag\left[\frac{\epsilon_u}{\epsilon_u - \epsilon_t}\right] \tag{19}$$

where f_t, ϵ_u and ϵ_t are illustrated in Figure 4. The scalar κ in equation (15) is defined as

$$\kappa = \sqrt{\left(\frac{\epsilon_I}{\epsilon_{tI}}\right)^{\frac{\alpha}{2}} + \left(\frac{\epsilon_{II}}{\epsilon_{tII}}\right)^{\frac{\alpha}{2}}} - 1 \tag{20}$$

Damaging is assumed to occur for $\kappa > 0$, and the material is considered not to take any load when the D_{ii} terms exceed unit.

It has been analytically shown that the linear mixed mode formulation is satisfied if

$$\begin{aligned} \epsilon_{tI} &= \epsilon_{tII} \\ \bar{\epsilon}_{II} &= p\,\bar{\epsilon}_I \end{aligned} \tag{21}$$

which implies a proportional straining. It has been proposed that α be left as a user parameter, which can take non-integer values between 2 and 4 to obtain an interaction relationship lying between a linear and a quadratic mixed mode [12].

4.3 Crack Direction

For material fracture, the genral anisotropic Tsai-Wu or Hoffman criteria do not provide any information regarding the crack direction. A simple popular method is according to the maximum principal stress (or strain) direction which can be similarly adopted in 3D applications

A far more sophisticated method for determining the crack direction is the so called acoustic tensor method, which was initially established for wave propagation problem in

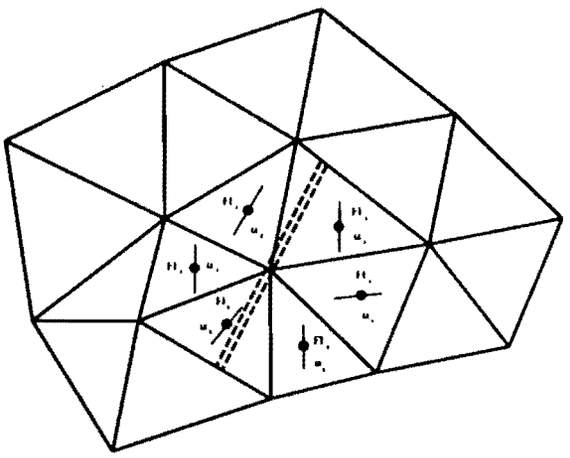

Figure 6: Weighted averaging of the failure indicator and the crack direction for a failed point.

solids. In this method, it is proved that the discontinuity plane satisfies the acoustic tensor equation,

$$detQ = det\,(\boldsymbol{n} \cdot \boldsymbol{D}_{el} \cdot \boldsymbol{n}) = 0 \tag{22}$$

where $\boldsymbol{Q}$ is often referred to as the acoustic or characteristic tensor, $\boldsymbol{D}_{el}$ is the elastoplastic consistent tangent matrix, and the orientation of the discontinuity plane is described by the normal $\boldsymbol{n}$. The closed form solution may only be derived for two dimensional problems and a simple iterative approach is required to solve equation (22) for $\boldsymbol{n}$ [13].

4.4 Remeshing Technique

Material fracture may result in the creation of new discrete bodies which are in contact by friction interaction with neighbouring bodies. A special remeshing algorithm is adopted to maintain compatibility conditions in newly fractured regions.

The failure indicator and the crack direction for each individual element are evaluated from the material softening model. A weighted averaging scheme is then used to evaluate both the failure indicator and the average crack direction of each node. Figure 6 illustrates this scheme for a two dimensional problem.

The next step is to geometrically represent the crack and perform the necessary split, separation and the remeshing processes. Figure 7 represents the two dimensional remeshing algorithm which comprises four steps: splitting the element, separating the failed nodes, creating new remeshing nodes, and dividing uncracked elements to enforce compatibility at new nodes. Adopting this local remeshing algorithm will provide a relatively finer mesh in the fractured region and prevents the distortion of the elements in this region, improving the finite element approximation of the analysis.

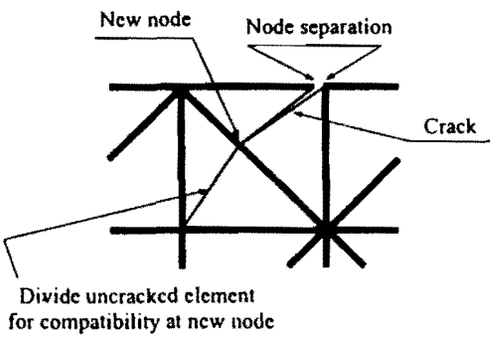

Figure 7: Remeshing scheme for modelling of fracture at a failed point.

5 Numerical Simulations

The author and his colleagues have previously published a number of papers verifying the method and providing several numerical simulations [2, 3, 14]. In this section the results of two other interesting dynamic fracturing problems are provided. Due to the limitiations on the length of the paper, for other details see references [14, 2].

5.1 Penetration of a missile into a ceramic plate

In this test, a missile is fired against a ceramic plate and penetrates through the plate. Figure 8 illustrates the crack patterns within the plate in different timesteps. This simulation is usually used in testing bullet proof devices.

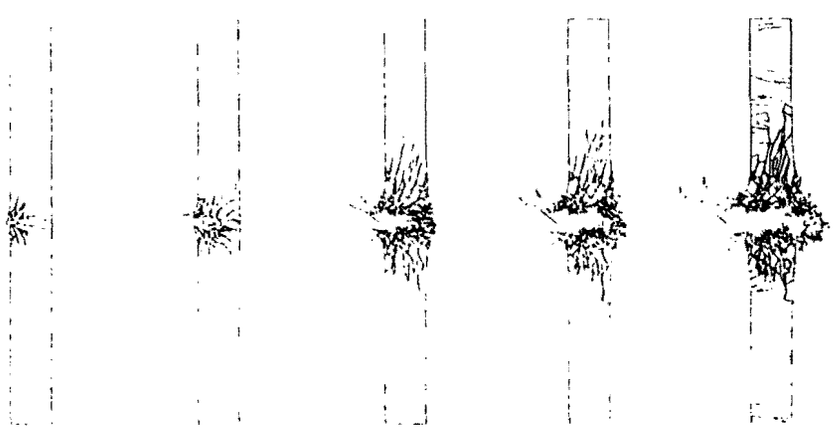

Figure 8: Progressive fracturing in a structure impacted by a high velocity bullet.

5.2 Demolition of a chimney tower due to a base explosion

Detonating a small mass of explosive material has cuased progressive fragmentation in a classic chimney tower as illustrated in Figure 9. Here, a gas-solid interaction algorithm is also used to allow for accurate modelling of variable gas pressure during the explosion and large deformation of the structure. The details of the method is out of scope of this paper and will be provided separately.

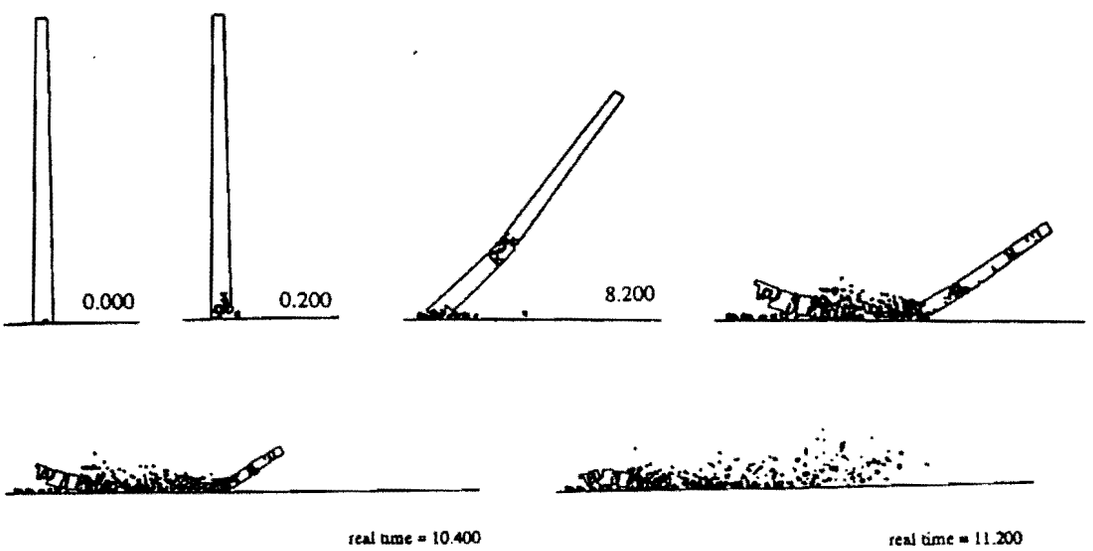

Figure 9: Demolition of a chimney tower subjected to explosive loading.

6 Conclusions

The combined finite/discrete element has proved to be an efficient algorithm for dealing with multi-fracture and fragmentation processes, which frequently arise from impact loadings on structures. An alternating digital tree method is adopted to reduce the extensive numerical costs of the contact detection phase. A local remeshing scheme is introduced for geometric modelling of the cracks, which plays an important role in avoiding the excess distortions of the finite elements in the vicinity of cracks. Numerical simulations of practical problems have been used to assess the performance of the method.

Acknowledgements

This work has been supported by Farinkav Engineering Research Company, which is gratefully acknowledged. The author would also like to appreciate the Department of Civil Engineering, University of Tehran for providing the necessary computing facilities.

References

[1] A. Munjiza, D.R.J. Owen, N. Bicanic. A combined finite-discrete element method in transient dynamics of fracturing solids. *Engineering Computations*, **12**:145–174, 1995.

[2] S. Mohammadi, D.R.J. Owen, D. Peric. Discontinuum approach for damage analysis of composites. In M.A. Crisfield, editor, *Computational Mechanics in UK - 5th ACME Conference*, pages 40–44, April 1997. London, UK.

[3] S. Mohammadi, D.R.J. Owen, D. Peric. A combined finite/discrete element algorithm for delamination analysis of composites. *Finite Elements in Analysis and Design*, **28**:321–336, 1998.

[4] M. Schonauer, T.Rodic, D.R.J. Owen. Numerical modelling of thermomechanical processes related to forming operations. *Journal De Physique IV*, **3**:1199–1209, 1993.

[5] J.C.J. Schellekens, R. de Borst. The use of hoffman yield criterion in finite element analyses of anisotropic composites. *Computers and Structures*, **37**(6):1087–1096, 1990.

[6] M.A. Crisfield. *Non-linear Finite Element Analysis of Solids and Structures. Volume 2: Advanced Topics*. John Wiley & Sons Ltd., 1997.

[7] D.R.J. Owen, A.J. Fawkes. *Engineering Fracture Mechanics*. Pineridge Press, 1983.

[8] G.T. Camacho, M. Ortiz. Adaptive lagrangian modelling of ballistic penetration of mettalic targets. *Computer Methods in Applied Mechanics and Engineering*, **142**:269 301, 1997.

[9] A.J.L. Crook. Combined finite/ discrete element method. Lecture Notes, Dept. of Civil Engineering, University of Wales Swansea, 1996.

[10] A.J. Kinloch, Y. Wang, J.G. Williams, P. Yayla. The mixed-mode delamination of fiber composite materials. *Composite Science and Technology*, **47**:225–237, 1993.

[11] A.S.D. Wang. Fracture analysis of interlaminar cracking. In N.J. Pagano, editor, *Interlaminar Response of Composite Materials*, chapter 2, pages 69–149. Elsevier Science Publishers B.V., 1989.

[12] Y. Mi, M.A. Crisfield. Analytical derivation of load/displacement relationship for the dcb and mmb and proof of the fea formulation. Ic-aero report 97-02 issn 0308-7247, Aeronautics Department, Imperial College of Science, Technology and Medicine, 1996.

[13] C.J. Pearce. *Computational Plasticity in Concrete Failure Mechanics*. PhD thesis, Department of Civil Engineering, University of Wales Swansea, 1996.

[14] D.R.J. Owen, D. Peric, S. Mohammadi. Discrete element modelling of multi-fracturing solids and structures. In *Foreign Object Impact and Energy Absorbing Structure*, pages 47–64. IMechE. 1998. London.